RESEARCH ARTICLE

Metabolic Correlates of Dopaminergic Loss in Dementia With Lewy Bodies

Maria Huber,[1] Leonie Beyer, MD,[1] Catharina Prix, MD,[2] Sonja Schönecker, MD,[2] Carla Palleis, MD,[2] Boris-Stephan Rauchmann, MD,[3,4] Silvia Morbelli, MD, PhD,[5,6] Andrea Chincarini, PhD,[7] Rose Bruffaerts, MD, PhD,[8,9] Rik Vandenberghe, MD,[8,9] Koen Van Laere, MD,[10] Milica G. Kramberger, MD, PhD,[11] Maja Trost, MD,[11,12] Marko Grmek, MD,[12] Valentina Garibotto, MD,[13] Nicolas Nicastro, MD,[14,15] Giovanni B. Frisoni, MD,[16] Afina W. Lemstra, MD, PhD,[17] Jessica van der Zande, MSc,[17] Andrea Pilotto, MD,[18,19] Alessandro Padovani, MD, PhD,[18] Sara Garcia-Ptacek, MD, PhD,[20,21] Irina Savitcheva, MD, PhD,[22] Miguel A. Ochoa-Figueroa, MD, PhD,[23,24,25] Anette Davidsson, PhD,[23] Valle Camacho, MD, PhD,[26] Enrico Peira,[7,27] Dario Arnaldi, MD, PhD,[5,27] Matteo Bauckneht, MD,[5,6] Matteo Pardini, PhD,[5,27] Gianmario Sambuceti, MD,[5,6] Jonathan Vöglein, MD,[2,28] Jonas Schnabel,[1] Marcus Unterrainer, MD,[1] Robert Perneczky, MD,[3,28,29,30] Oliver Pogarell, MD,[3] Katharina Buerger, MD,[28,30] Cihan Catak, MD,[30] Peter Bartenstein, MD,[1,31] Paul Cumming, PhD,[32,33] Michael Ewers, MD,[28] Adrian Danek, MD,[2] Johannes Levin, MD,[2,28,31] Dag Aarsland, MD,[34,35] Flavio Nobili, MD,[5,27] Axel Rominger, MD,[1,31,32] and Matthias Brendel, MD[1,31*]

[1]*Department of Nuclear Medicine, University Hospital of Munich, LMU Munich, Munich, Germany*
[2]*Department of Neurology, University Hospital of Munich, LMU Munich, Munich, Germany*
[3]*Department of Psychiatry and Psychotherapy, University Hospital, LMU Munich, Munich, Germany*
[4]*Department of Radiology, University Hospital of Munich, LMU Munich, Munich, Germany*
[5]*IRCCS Ospedale Policlinico San Martino, Genoa, Italy*
[6]*Nuclear Medicine Unit, Department of Health Sciences, University of Genoa, Genoa, Italy*
[7]*National Institute of Nuclear Physics (INFN), Genoa section, Genoa, Genoa, Italy*
[8]*Department of Neurosciences, Faculty of Medicine, KU Leuven, Leuven, Belgium*
[9]*Department of Neurology, University Hospitals Leuven, Leuven, Belgium*
[10]*Department of Nuclear Medicine, University Hospitals Leuven, Leuven, Belgium*
[11]*Department of Neurology, University Medical Centre, Ljubljana, Slovenia*
[12]*Department for Nuclear Medicine, University Medical Centre, Ljubljana, Slovenia*
[13]*Division of Nuclear Medicine and Molecular Imaging, Geneva University Hospitals and NIMTLab, Geneva University, Geneva, Switzerland*
[14]*Department of Clinical Neurosciences, Geneva University Hospitals, Geneva, Switzerland*
[15]*Department of Psychiatry, University of Cambridge, Cambridge, United Kingdom*
[16]*LANVIE (Laboratoire de Neuroimagerie du Vieillissement), Department of Psychiatry, Geneva University Hospitals, Geneva, Switzerland*
[17]*VU Medical Center Alzheimer Center, Amsterdam, The Netherlands*
[18]*Neurology Unit, University of Brescia, Brescia, Italy*
[19]*Parkinson's Disease Rehabilitation Centre, FERB ONLUS–S. Isidoro Hospital, Trescore Balneario (BG), Italy*
[20]*Division of Clinical Geriatrics, Center for Alzheimer Research, Department of Neurobiology, Care Sciences and Society, Karolinska Institutet, Stockholm, Sweden*
[21]*Internal Medicine, section for Neurology, Sädersjukhuset, Stockholm, Sweden*
[22]*Medical Radiation Physics and Nuclear Medicine, Karolinska University Hospital, Stockholm, Sweden*
[23]*Department of Clinical Physiology, Institution of Medicine and Health Sciences, Linköping University Hospital, Linköping, Sweden*
[24]*Department of Diagnostic Radiology, Linköping University Hospital, Linköping, Sweden*
[25]*Center for Medical Image Science and Visualization (CMIV), Linköping University, Linköping, Sweden*
[26]*Servicio de Medicina Nuclear, Hospital de la Santa Creu i Sant Pau, Universitat Autònoma de Barcelona, Barcelona, España*
[27]*Clinical Neurology, Department of Neuroscience (DINOGMI), University of Genoa, Genoa, Italy*
[28]*DZNE–German Center for Neurodegenerative Diseases, Munich, Germany*
[29]*Ageing Epidemiology Research Unit (AGE), School of Public Health, Imperial College, London, United Kingdom*

***Correspondence to:** Dr. Matthias Brendel, Department of Nuclear Medicine, University Hospital of Munich, Marchioninistraße 15, 81377 Munich, Germany; E-mail: matthias.brendel@med.uni-muenchen.de

Ms. Huber and Dr. Beyer contributed equally to this work.

Relevant conflicts of interest/financial disclosures: Nothing to report.

Full financial disclosures and author roles may be found in the online version of this article.

Received: 7 August 2019; **Revised:** 21 October 2019; **Accepted:** 23 October 2019

Published online 16 December 2019 in Wiley Online Library (wileyonlinelibrary.com). DOI: 10.1002/mds.27945

[30]Institut for Stroke and Dementia Research, University of Munich, Munich, Germany
[31]Munich Cluster for Systems Neurology (SyNergy), Munich, Germany
[32]Department of Nuclear Medicine, University of Bern, Inselspital, Bern, Switzerland
[33]School of Psychology and Counselling and IHBI, Queensland University of Technology, Brisbane, Australia
[34]Centre for Age-Related Medicine (SESAM), Stavanger University Hospital, Stavanger, Norway
[35]Wolfson Centre for Age-Related Diseases, King's College London, London, United Kingdom

ABSTRACT: Background: Striatal dopamine deficiency and metabolic changes are well-known phenomena in dementia with Lewy bodies and can be quantified in vivo by ^{123}I-Ioflupane brain single-photon emission computed tomography of dopamine transporter and ^{18}F-fluorodesoxyglucose PET. However, the linkage between both biomarkers is ill-understood.
Objective: We used the hitherto largest study cohort of combined imaging from the European consortium to elucidate the role of both biomarkers in the pathophysiological course of dementia with Lewy bodies.
Methods: We compared striatal dopamine deficiency and glucose metabolism of 84 dementia with Lewy body patients and comparable healthy controls. After normalization of data, we tested their correlation by region-of-interest–based and voxel-based methods, controlled for study center, age, sex, education, and current cognitive impairment. Metabolic connectivity was analyzed by inter-region coefficients stratified by dopamine deficiency and compared to healthy controls.
Results: There was an inverse relationship between striatal dopamine availability and relative glucose hypermetabolism, pronounced in the basal ganglia and in limbic regions. With increasing dopamine deficiency, metabolic connectivity showed strong deteriorations in distinct brain regions implicated in disease symptoms, with greatest disruptions in the basal ganglia and limbic system, coincident with the pattern of relative hypermetabolism.
Conclusions: Relative glucose hypermetabolism and disturbed metabolic connectivity of limbic and basal ganglia circuits are metabolic correlates of dopamine deficiency in dementia with Lewy bodies. Identification of specific metabolic network alterations in patients with early dopamine deficiency may serve as an additional supporting biomarker for timely diagnosis of dementia with Lewy bodies.

Key Words: dopamine deficiency; glucose metabolism; Lewy body dementia; metabolic connectivity; PET imaging

Dementia with Lewy bodies (DLB) is the second-most common type of late-onset degenerative dementia,[1,2] which is characterized clinically by its core symptoms: fluctuations in cognition and alertness, parkinsonism, visual hallucinations, and rapid eye movement (REM) sleep behavior disorder. According to the accepted diagnostic criteria, DLB should be suspected when onset dementia occurs before or concurrently with parkinsonism.[3,4] The complex clinical picture of DLB renders its diagnosis challenging, especially at an early disease stage.[3,5] For this reason, molecular biomarkers, in particular dopamine transporter imaging by ^{123}I-Ioflupane brain single-photon emission computed tomography (DaT-SPECT) and ^{18}F-fluordeoxyglucose brain PET (FDG-PET), are now accepted tools supporting a diagnosis of DLB.[3,6,7]

Nigrostriatal degeneration, as indicated by reduced striatal DaT-SPECT binding, can distinguish DLB at an early disease stage from other neurodegenerative conditions, especially Alzheimer's disease (AD).[8,9] A previous study showed that reduced DaT-SPECT binding in the posterior putamen provides highly sensitive differential diagnosis of DLB.[10] An incomplete nigrostriatal dopaminergic degeneration is detectable by DaT-SPECT, even though parkinsonian motor symptoms are not yet conspicuous to clinical examination.[3,11]

FDG-PET provides a surrogate measure of neuronal injury, which can support a diagnosis of DLB by revealing region-specific patterns of altered glucose metabolism.[3,12] Our consortium recently investigated metabolic patterns and their covariance with clinical core features in the hitherto largest cohort of DLB patients undergoing molecular imaging, in a study within the framework of the European DLB (E-DLB) Consortium.[5].Extending beyond regional changes in metabolism, network analysis of FDG-PET revealed altered patterns of metabolic connectivity between different brain regions.[13] One such FDG-PET study in DLB patients showed patterns of perturbed metabolic connectivity involving cholinergic and dopaminergic pathways and in association with the spreading synucleinopathy occurring in DLB.[14] However, studies using functional MRI (fMRI) have provided inconsistent evidence for increasing, decreasing, or unaltered functional connectivity in different brain regions or functionally related neuronal circuits in DLB

patients compared to healthy controls (HCs) and/or AD patients.[15-19]

Although both DaT-SPECT and FDG-PET are now well-established procedures for indicative or supportive diagnosis of DLB, there is only limited documentation of the covariance of the two biomarkers. In Parkinson's disease (PD) and atypical parkinsonian syndromes, metabolic network expression and dopamine availability were found to provide complementary information underlying the disease process.[20,21] Although there are several studies investigating the relationships of these two biomarkers' relationship in PD,[21,22] corresponding results are available in only in a few DLB cases so far.[20,23] Therefore, we undertook to evaluate the relationship between individual dopamine deficiency and altered glucose metabolism in a well-powered, cross-sectional analysis of our large multicenter E-DLB cohort. First, we correlated individual dopamine deficiency as indicated by DaT-SPECT with striatal glucose metabolism measured by FDG-PET. We then undertook regional and voxel-wise analyses to investigate the association between the two biomarkers throughout the brain. Finally, we calculated metabolic connectivity as a function of the extent of dopamine deficiency.

Materials and Methods

Research Project, Conception, Design, and Patient Selection

We took advantage of the framework of the E-DLB consortium that had agreed to share clinical and imaging data from patients with DLB,[24] including recently published findings of the project's FDG-PET arm.[25] From the 189 patients with an available anonymized brain FDG-PET scan from nine centers, we assembled the 89 patients with additional DaT-SPECT images in their original Digital Imaging and Communications in Medicine (DICOM) format. Five patients were excluded because of insufficient demographic data (see a previous work[25]), resulting in 84 included subjects. Age-matched DaT-SPECT images of 37 historical HCs from a previously published, multicenter study[26] and FDG-PET images of 28 HCs imaged in Genova and Munich (14 each) served as control material.

Local institutional ethics committee approvals for the retrospective analyses were available for all centers, including the transfer of imaging data. Patients gave informed written consent for the imaging procedure and radiopharmaceutical application.

DaT-SPECT and FDG-PET Procedure and Preprocessing

We compiled the DaT-SPECT DICOM files and evaluated them with Hermes HybridBRASS using the standard settings for this analysis. Correction for age was included in the generation of Z-score values against the corresponding HC data. We calculated the DaT ratio in the bilateral putaminal volumes of interest (VOIs) as defined in BRASS model 5, relative to uptake in the bilateral occipital lobe reference region.

FDG-PET preprocessing for all subjects was performed in Munich according to procedures established in the previous E-DLB work.[25] In brief, the original FDG-PET DICOM image files were spatially normalized (nonlinear warping; transient input filter 8 mm^3; 16 iterations; frequency cutoff 3; regularization 1.0; no thresholding) with PMOD (V3.5; PMOD Technologies, Basel, Switzerland) to an FDG-PET template. Individual images were intensity normalized to their global mean and then smoothed using a Gaussian filter (8 mm^3) to obtain maps of FDG uptake as standardized uptake value ratios (SUVrs) in 77 predefined cortical and subcortical gray matter VOIs of the Hammers atlas[27] after exclusion of the ventricular system and the corpus callosum. Brain regions other than insula, cerebellum, and pons were assigned to one of the following six structural or functional compartments: frontal cortex, parietal cortex, temporal cortex, occipital cortex, limbic system, and basal ganglia. The putamen uptake represented the extended striatum, given that VOI placement in the caudate nucleus tended to impinge upon the cerebral ventricles.

To evaluate potential quantification bias of relative glucose metabolism increases arising from the normalization method, we also reprocessed all data by scaling to cerebellar gray matter values and a cluster-based normalization. Corresponding results are presented online (see Supporting Information Fig. 1). The reference cluster was determined by similarity analysis (voxels ≤2% deviation) between DLB patients and HCs.[28] Values deriving from global mean scaling were used for further analyses. Data were visually checked for image quality after each process step. The mean time interval between FDG-PET and DaT-SPECT imaging was $+3.0 \pm 4.8$ months. Disease duration was the elapsed time between the first symptoms of the patients and the date of scanning.

Statistical Analysis

Statistical tests were performed using SPSS (V25.0; IBM Corp., Chicago, IL) and statistical parametric mapping (SPM; V12; Functional Imaging Laboratory, The Wellcome Trust Centre in the Institute of Neurology, University College of London, London, UK) running in Matlab (version R2016a; The MathWorks, Inc., Natick, MA). We tested normality of data distribution for DaT ratios and all regional FDG-PET SUVr measurements with the Kolmogorov-Smirnov test. Putamen DaT ratios and regional FDG-PET SUVrs in the putamen were compared between the DLB patient and

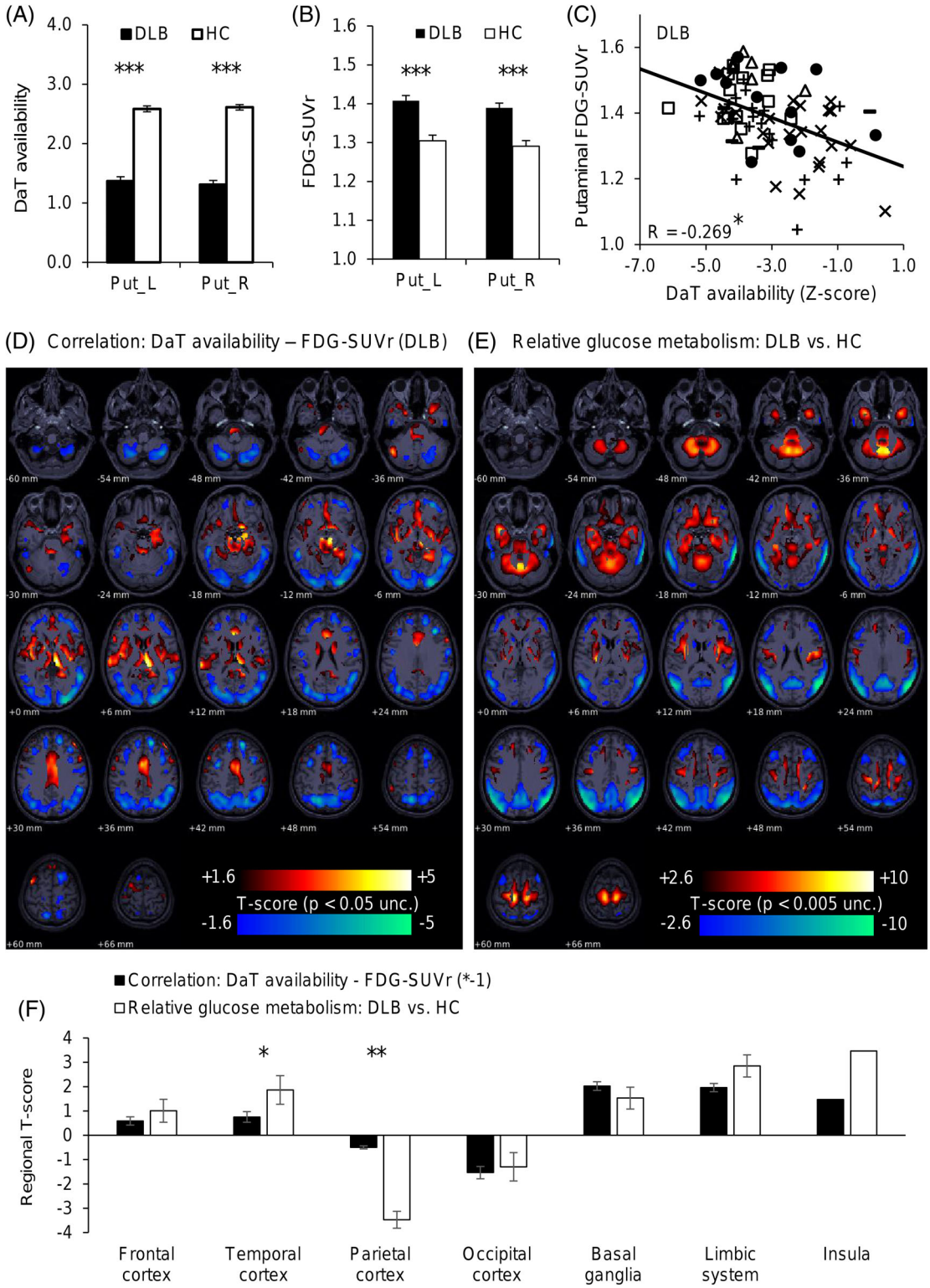

FIG. 1. VOI and voxel-based associations of DaT availability and relative glucose metabolism. (**A**) Put_L/R, left/right putamen. (**B**) FDG SUVr, relative glucose metabolism. (**C**) Different symbols indicate different centers. (**D**) Clusters of negative/positive (red/ blue) associations (predictor DaT availability, outcome variable and relative glucose metabolism). (**E**) Clusters of relative hypo-/hypermetabolism (blue/red; DLB vs. HC). (**F**) Quantitative comparison of associations between DaT availability and relative glucose metabolism (black bars) and the disease-related pattern of DLB patients when compared to HCs (white bars) for different brain regions. The average values (±SD [standard deviation]) of regional T-scores deriving from SPM are given for each brain region. $^{*}P < 0.05$; $^{**}P < 0.01$, error bars indicate SDs. Brain regions in D/E are masked by a gray matter atlas. [Color figure can be viewed at wileyonlinelibrary.com]

HC groups by an unpaired Student's *t* test. A significance level of $P < 0.05$ was applied in all analyses.

Correlation Analyses

Pearson's coefficient of correlation (R) for the two biomarkers in the putamen was calculated after adjusting for center, subject age, sex, education level, and disease duration. A subgroup of 70 DLB patients also allowed correction for current cognitive impairment as assessed by the Mini-Mental State Examination (MMSE) score. Associations between each subject's DaT Z-score and FDG-PET SUVr in all predefined brain regions were characterized by applying linear regression analyses. All values were adjusted for age (n = 84), sex (n = 84), education (n = 84), disease duration (n = 84), and MMSE (n = 70) by linear regression before the analysis. We applied a strict Bonferroni correction to account for multiple comparisons of the 77 brain regions.

Voxel-wise Analyses

Voxel-wise statistical analyses were performed using SPM12. A regression analysis was performed using putamen DaT Z-Scores as predictor and voxel-wise FDG-PET SUVr as outcome variable, with imaging center, subject age, sex, and education level as covariates (SPM threshold $P < 0.05$, uncorrected [unc.]). Additionally, we made a voxel-wise contrast of FDG-PET SUVr images of DLB patients versus HCs using an unpaired *t* test and compared regional t-scores between the regression analysis and the contrast against HCs (SPM threshold $P < 0.005$, unc.). Binarized SPM maps were tested for similarity by calculation of Dice coefficients as previously described.[29]

Metabolic Connectivity

We assessed metabolic connectivity from inter-regional coefficients of FDG-PET SUVr for DLB patients at different stages of dopamine deficiency and for the HC group, as initially described by Horwitz and colleagues.[30] For this purpose, regional FDG-PET values of all 77 brain regions were extracted after normalization to global mean, and an inter-region correlation matrix of 77×77 Pearson's correlation coefficients was created for each analyzed group.

The DLB cohort was stratified by tertiles of 28 subjects each with severe, intermediate, and mild dopamine deficiency to the DaT-SPECT Z-Score (age/sex not statistically different). Thus, we performed the connectivity analysis in these three subgroups and a group of 28 age-matched HCs to avoid statistical biases attributed to differing sample sizes. Single inter-region coefficients of different brain areas were compared between the resulting four groups by analysis of variance, including Bonferroni correction for the number of coefficients studied and the number of subgroups. Fisher's R to Z transformation was performed for all values to enhance normal distribution. A significance level of $P < 0.05$ after Bonferroni correction was applied in all analyses. Furthermore, the regional regression coefficients between DaT Z-Score and FDG-PET SUVr in putamen were correlated with mean loss of connectivity in the corresponding investigated brain regions defined as the difference (delta) between DLB and HCs, calculated by subtracting values of each inter-region coefficient.

Results

Associations Between Dopamine Deficiency and Relative FDG Uptake

Demographics and disease parameters of the DLB cohort and our historical HC groups are presented in Table 1. Our DLB cohort revealed a strongly reduced dopamine transporter availability in bilateral putamen (–48%, $P < 0.001$, *t* test; Fig. 1A) and significantly higher relative glucose metabolism rates (+7.5%, $P < 0.001$, *t* test; Fig. 1B) in the bilateral putamen when compared to the age-matched HC group. Importantly, there was a negative association between DaT Z-scores and FDG-PET SUVr in the putamen after controlling for imaging center, subject age, sex, and education ($R = -0.269$; $P = 0.016$, partial correlation; Fig. 1C). The two imaging biomarkers were still significantly associated after additional controlling for disease duration ($R = -0.253$; $P = 0.030$, partial correlation). Furthermore, this association remained stable in the 70 cases where MMSE score was available to control for current cognitive impairment, together with the usual adjustment for age, sex, and education ($R = -0.318$; $P = 0.009$, partial correlation), compared to only adjusting for age, sex, and education in that subgroup ($R = -0.322$; $P = 0.008$, partial correlation). We

TABLE 1. Demographics and composition of the study collective

	DLB	HC (FDG-PET)	HC (DaT-SPECT)
N	84	28	37
Age (y)	72.6 ± 7.0	73.2 ± 7.6	70.1 ± 6.0
Sex (♂/♀)	47♂ 37♀	17♂ 11♀	21♂ 16♀
MMSE (0–30)	22.6 ± 4.3		
Education (y)	12.1 ± 3.7		
Disease duration (y)	2.7 ± 2.0		
Parkinsonism	82%		
Visual hallucinations	65%		
Fluctuating cognition	73%		
REM sleep behavior disorder	49%		
Possible DLB[a]	26%		
Probable DLB[a]	74%		

[a]McKeith criteria of 2017.[3]
N, number of subjects; y, years.

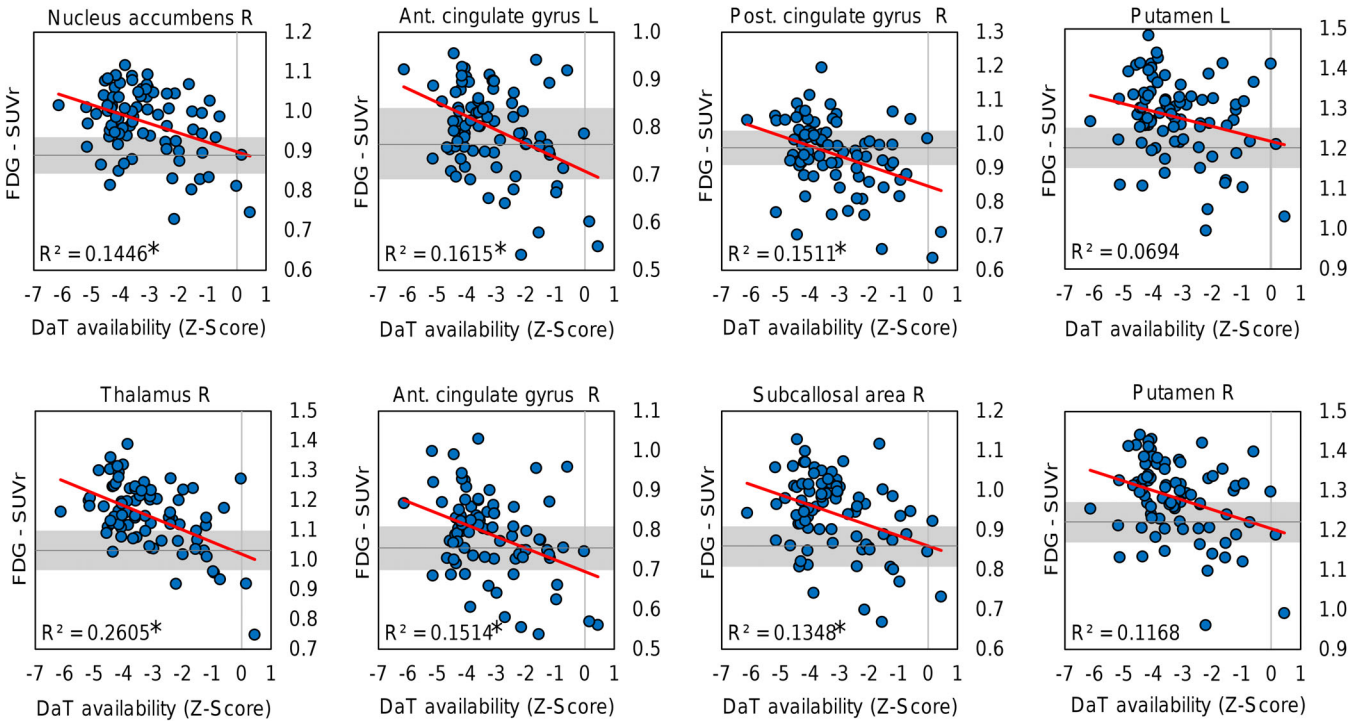

FIG. 2. Region-based associations of dopamine transporter availability and relative glucose metabolism. The range of FDG-SUVr values of healthy controls ± standard deviation indicated in gray. Significant associations (after Bonferroni correction) of 6 of 77 tested regions are indicated with an asterisk ("*").DaT, putaminal dopamine transporter. R, right. L, left. FDG-SUVr, relative glucose metabolism. [Color figure can be viewed at wileyonlinelibrary.com]

could not control for study center in combination with MMSE because of the heterogeneous MMSE distribution across study centers.

Compared to HCs, the DLB-related pattern (DLBRP) in FDG-PET showed a relatively reduced metabolism in the parietal, occipital, and, to a lesser extent, frontal cortices and a relative hypermetabolism in the basal ganglia, parts of the limbic system, the motor cortices, and the cerebellum (Fig. 1E).

The voxel-wise regression analysis revealed clusters showing a negative correlation between both biomarkers, which was most conspicuous in the basal ganglia and limbic system, that is, the putamen, thalamus, SN, and anterior and posterior cingulate gyrus (Fig. 1D, red). Clusters with positive associations were observed in parietal and occipital cortices as well as in the cerebellum (Fig. 1D, blue). Negative correlation clusters in the basal ganglia and limbic system overlapped with regions of general increases within the DLBRP (Dice similarity: 24%; Fig. 1E,F). The positive correlation clusters in the occipital cortex overlapped with regions of generally reduced relative glucose metabolism within the DLBRP (Dice similarity: 41%; Fig. 1E,F). Relative FDG uptake in the parietal cortex showed only a weak positive correlation with dopamine deficiency, but this cortical region revealed the strongest decrease of relative glucose metabolism within the DLBRP (Fig. 1F). Relative increases of glucose metabolism in temporal regions were accompanied by weak correlations with nigrostriatal dopamine degeneration (Fig. 1F). There were only minor overlaps between negative correlation clusters and reduced relative glucose metabolism in DLB (Dice similarity: 3%) and between positive correlation clusters and increased relative glucose metabolism in DLB (Dice similarity: 8%).

Next, we applied region-based linear regression of FDG uptake as a function of DaT Z-Scores for all 77 brain regions with correction for multiple comparisons (Fig. 2) after adjustment for age, sex, education, disease duration, and current cognitive function. Notably, only negative significant associations were observed: in the right nucleus accumbens (R = –0.380; $F_{2,81}$ = 13.9; P = 0.028), the right thalamus (R = –0.510; $F_{2,81}$ = 28.9; P = 0.0001), the bilateral anterior cingulate gyrus (R = –0.402/–0.389; $F_{2,81}$ = 15.8/14.6; P = 0.012/0.020), the right posterior cingulate gyrus (R = –0.389; $F_{2,81}$ = 14.6; P = 0.020), and the right subcallosal area (R = –0.367; $F_{2,81}$ = 12.8; P = 0.046; Fig. 2). The other brain regions did not show significant correlations. The initially observed direct association in the putamen did not survive correction for multiple comparisons (Fig. 2).

Metabolic Connectivity at Different Stages of Dopamine Deficiency in DLB

Metabolic connectivity was analyzed in three subgroups of DLB patients of the same size (28 subjects each) stratified according to their degree of dopamine

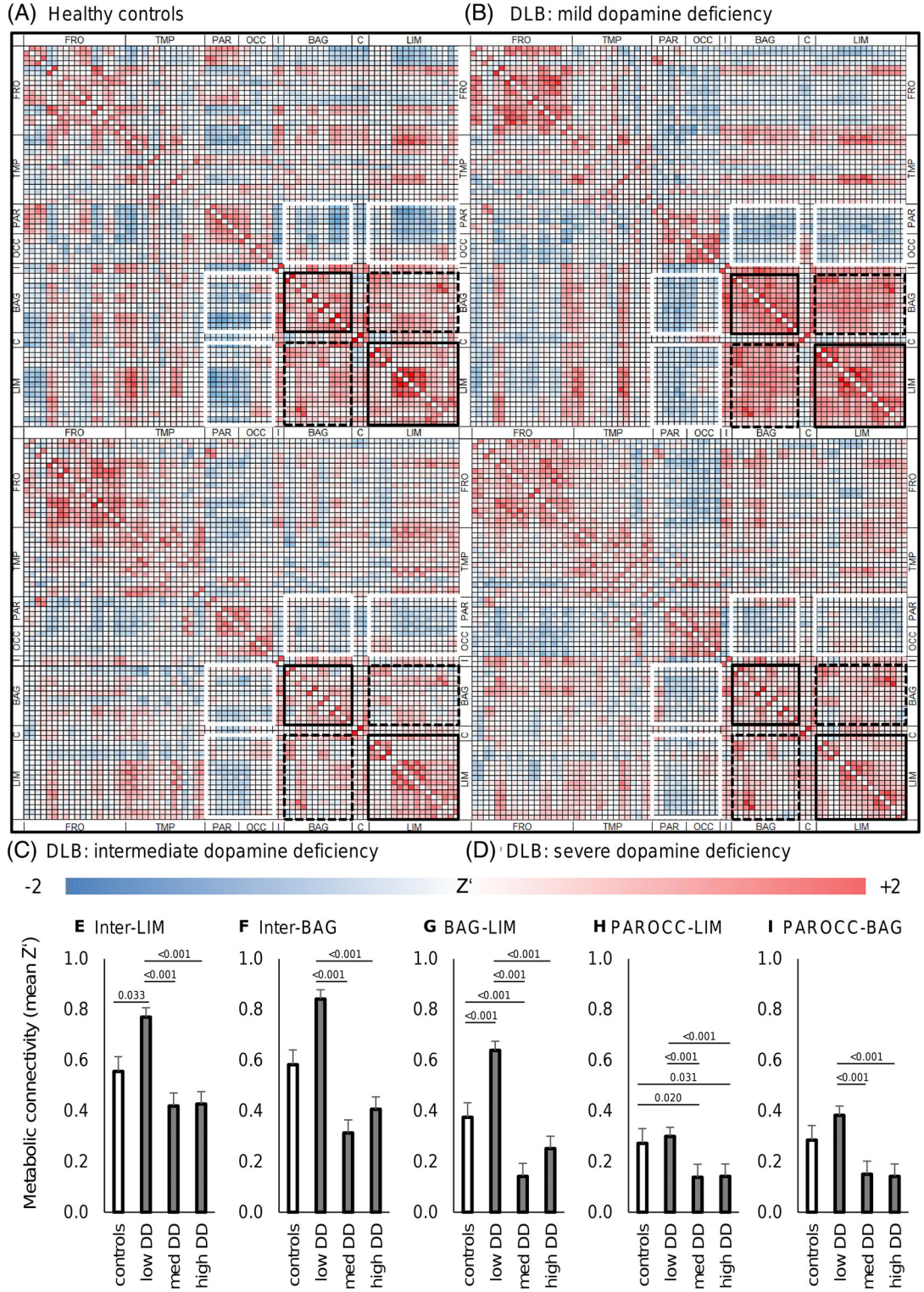

FIG. 3. Metabolic connectivity at different stages of dopaminergic loss, as indexed by DaT SPECT. (**A–D**) Single boxes indicate inter-regional Z'. Regions with significant differences between groups are highlighted with black, black-dotted, and white lines. (**E–I**) DD = dopamine depletion to DaT SPECT. Error bars indicate standard deviations. FRO, frontal cortex; TMP, temporal cortex; PAR, parietal cortex; OCC, occipital cortex; I, insula; BAG, basal ganglia; C, cerebellum and brainstem; LIM, limbic structures. [Color figure can be viewed at wileyonlinelibrary.com]

deficiency (mild, mean DaT Z-Score of -1.6 ± 0.9; intermediate, mean DaT Z-Score of -3.5 ± 0.3; severe, mean DaT Z-Score of -4.5 ± 0.5) and compared to that in a size- and age-matched HC group (28 subjects) with presumably intact nigrostriatal dopamine innervation (Fig. 3A–D).

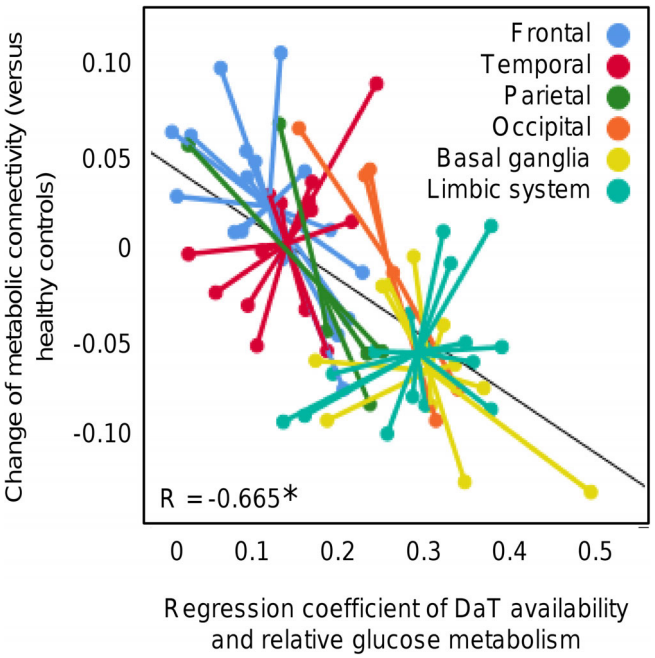

FIG. 4. Association between relative regional hypermetabolism and loss of connectivity. DaT, putaminal dopamine transporter. Regression coefficient (association analysis of DaT availability and relative glucose metabolism; Fig. 2). Change of metabolic connectivity (Δ mean Z' vs. healthy controls; Fig. 3). [Color figure can be viewed at wileyonlinelibrary.com]

Strikingly, the strongest alterations of metabolic connectivity in comparison to HCs were observed within the limbic circuits and basal ganglia (see black boxes in Fig. 3A–D and 3E,F) and between the limbic circuit and basal ganglia (see black dotted boxes in Fig. 3A–D and 3G). The metabolic connectivity was increased in the DLB group with mild dopamine deficiency compared to age-matched HCs, but connectivity then fell significantly lower for DLB stages of intermediate or severe dopamine deficiency (Fig. 3E–G). We also observed a significant decrease of metabolic connectivity between parieto-occipital brain areas and the limbic system/basal ganglia, which was enhanced with increasing dopamine deficiency (see white boxes in Fig. 3A–D and 3H,I). Other brain areas showed no significant differences in metabolic connectivity.

Metabolic connectivity was significantly lower for regions with a higher association between dopamine deficiency and relative glucose metabolism ($R = -0.665$; $P < 0.01$; Fig. 4). Single regions clustered along their defined anatomical or functional compartments when plotting regression coefficients deriving from the association between dopamine deficiency and relative glucose metabolism together with connectivity changes. In summary, we observed a clear linkage between the relative hypermetabolism associated with dopaminergic loss and decreased metabolic connectivity at the regional level of DLB patients.

Discussion

We present the first large-scale investigation of the relationship between dopamine deficiency in the bilateral putamen and global perturbations of relative glucose metabolism in DLB patients. Our data provide evidence for an association between dopaminergic deficiency and increased relative glucose metabolism pronounced in the basal ganglia and limbic system, independent of disease duration, current cognitive impairment, and other common covariates. Metabolic connectivity in these same brain areas increases slightly at an early stage of dopamine deficiency, but deteriorates strongly when nigrostriatal degeneration is of intermediate or severe magnitude.

An extensive body of research documents the PD-related pattern (PDRP) of metabolism in relation to clinical and dopaminergic measures.[20,21] There was a significant inverse relationship between dopamine transporter availability in the striatum and PDRP expression, whereas neither extent of dopamine deficiency nor PDRP expression correlated strongly with disease duration or severity.[20] In our DLB cohort, region-based and voxel-wise correlation analyses also showed strong associations between dopamine deficiency and the disease-specific metabolic pattern of DLB. Notably, we found a significant correlation between dopamine deficiency in the putamen and increasing relative glucose metabolism throughout the bilateral striatum, resulting in an overall striatal hypermetabolism of DLB subjects compared to HCs. Until now, changes of striatal glucose metabolism have not been evaluated in detail with respect to the course of DLB, although the striatum is certainly vulnerable to DLB pathology.[8] In PD, it has been shown that the neuronal firing rate and synchrony of neurons in the dorsal striatum is altered along the course of disease progression, in concert with continuing dopamine deficiency.[31] This relationship may arise because of effects of a pacemaker center in the basal ganglia that compensates dopaminergic loss with increased neuronal firing and consequently increased metabolic activity.[32] Thus, our current findings in DLB could also reflect a compensatory or disinhibition mechanism whereby metabolism increases in the partially dopamine-depleted striatum. Importantly, the association between loss of dopamine innervation and relatively increasing glucose metabolism in the putamen remained after controlling for disease duration and current cognitive function, as indexed by the MMSE score.

Compared to the PDRP, the DLBRP measured in our study showed additional regions of relative hypometabolism in the occipital cortices and, even more important, additional regions of relative hypermetabolism in the limbic system. In comparison to PD, patients with DLB present with additional core symptoms like visual hallucinations and cognitive impairment arising from the more pronounced

cortical involvement. As we have observed, additional brain regions, such as the limbic system, also showed relative glucose hypermetabolism in the contrast between DLB patients and HCs and, furthermore, revealed a strong negative correlation with the extent of dopaminergic loss in the putamen (Fig. 1F). We speculate that increasing relative limbic glucose metabolism arises secondary to impaired dopaminergic signaling in the basal ganglia, perhaps attributable to disinhibition or as a compensatory response to decreasing signal input. This finding is of particular interest given that it may also harbor the molecular basis for the cingulate island sign in DLB, that is, the relative sparing of mid-posterior cingulate cortex metabolism.[33] Some areas with a negative correlation between putaminal DaT-SPECT and voxel-wise FDG-PET were observed in the white matter and near the ventricles. This probably spurious finding could be related to the presence of greater AD-like and vascular pathology in those DLB subjects with relatively preserved dopaminergic innervation, resulting in proportionately greater atrophy and white matter disease. Future imaging studies need to draw attention toward the impact of various existing copathologies in DLB on our observed association between dopaminergic loss in striatum and metabolic function in the brain.

To get a deeper insight into potential pathomechanisms resulting in perturbed glucose metabolism in DLB subjects, we investigated metabolic connectivity in FDG-PET by inter-region coefficient methods. Functional connectivity in DLB subjects has already been investigated in several fMRI studies.[15-19] Most of these fMRI studies investigated the discrepancies between DLB subjects and HC and/or AD subjects, while focusing on particular brain regions known to be affected in the respective diseases. As we have demonstrated in the present study, some of the discrepant findings of those fMRI studies may arise from reporting connectivity alterations without adjustment for the stage of dopaminergic loss of the included DLB subjects. In our cohort, the combined analysis of dopamine deficiency and relative glucose metabolism offers the opportunity to investigate metabolic connectivity as a function of dopaminergic loss. Stratified as mild/intermediate/severe dopamine degeneration, we found seemingly increased metabolic connectivity in limbic and basal ganglia regions at the early stage of dopaminergic loss compared to that in HCs (Fig. 3). Enhanced metabolic connectivity has already been reported between the right posterior cingulate cortex and other brain regions (inter alia the limbic system) in a previous study of DLB subjects.[16] With increasing nigrostriatal dopamine degeneration, the metabolic connections involving the basal ganglia and limbic system decreased and the metabolic connectivity of those brain regions was significantly lower than for DLB subjects with mild dopamine innervation loss in the putamen.

This finding supports the conjecture that relative hypermetabolism in the basal ganglia and limbic system in early DLB disease stages represents a disinhibition or compensatory mechanism, whereas impaired metabolic connectivity at later disease stages could reflect a breakdown or decompensation of the increasingly disturbed neuronal activity. Our findings are supported by one fMRI investigation, which found decreased functional connectivity in limbic and basal ganglia clusters of temporal and frontoparietal networks of a group of patients with advanced DLB.[17] An analogous compensatory recruitment hypothesis has already been proposed to occur in the course of AD.[34] In this scenario, connectivity initially increases because new brain areas are recruited, and impaired regions become hyperactive to compensate for functional loss in a process presenting as relative hypermetabolism to FDG-PET. The compensation process cannot be maintained when neurodegeneration proceeds past some point, whereupon decreasing metabolic connectivity is declared at this later disease stage. The seemingly dynamic changes of metabolic connectivity involving the limbic system might explain why relative FDG uptake did only partly differ in the voxel-wise analysis for the entire DLB group as compared to HCs (see Fig. 1).

Among the limitations of the study, we note that DLB diagnoses were obtained in different clinical settings and without histopathological verification. Furthermore, there might occur some selection bias into the direction of a more complex cohort of DLB patients in comparison to the general average in populations, given that patients evaluated by both imaging biomarkers had potentially a more conflicting clinical examination. Potential confounders, such as different cameras or nonstandardized enrollment of patients (clinical evaluation and examination), were minimized by inclusion of the imaging center as a covariate. Filtering of FDG-PET data was used to correct for possible spatial mismatch between subjects. Nonetheless, we cannot fully exclude the possibility of some remaining effects attributed to the multicenter design of this cross-sectional study.

The use of a global mean normalization may raise concerns about a potential artificial relative hypermetabolism attributed to a lower global glucose metabolism in subjects affected by DLB (i.e., causing a low denominator).[35,36] Although some research indicates absolute declines in cortical glucose consumption in patients with PD,[37] others report no significant difference between global glucose metabolism in PD patients compared to HCs, despite a focal increase of striatal metabolism.[38] Moreover, another study found a correlation between the changes of glucose metabolism in subcortical brain regions and motor function deterioration, which speaks against the interpretation that increased values are merely artefacts of the normalization process.[39] To strengthen this argument, we tested for the robustness of our findings of increased striatal glucose metabolism with normalization to other reference regions (see Supporting Information Fig. 1). Although there were

varying degrees of relative increase in the striatum, correlations of relative glucose metabolism with reduced DaT availability in the putamen remained stable. Thus, some areas with relatively increased glucose metabolism, such as the white matter of the bilateral frontal and parietal cortices, which might have been artifacts of the global mean normalization, did not significantly influence the present key results.

Our inter-region coefficient method represents a simplified model to assess metabolic or functional connectivity, which has previously revealed inter-regional correlations in an fMRI study.[40] However, our primary focus was to search for differences in metabolic connectivity as a function of the stage of putaminal dopaminergic loss in DLB. Therefore, we argue that a simple model is well suited to the task at hand. We note that FDG-PET has inherently lower spatial resolution compared to fMRI studies, but presume that functional connectivity operates for anatomical regions of the scale of our 77 atlas-based brain regions. FDG-PET has shown comprehensible results regarding the sufficient spatial resolution for metabolic connectivity analyses in AD subjects.[41] We note that the MMSE score certainly does not represent all aspects of disease severity in DLB. Unfortunately, to our knowledge, there is no widely accepted score to measure overall clinical severity in DLB. Therefore, MMSE was the only feasible, standardized index for use in this multicenter study.

Overall, we present the, so far, largest combined analysis of dopamine deficiency to DaT-SPECT imaging and widespread cerebrometabolic changes to FDG-PET in the same DLB subjects. Our data indicate a strong interrelation, with a pronounced association of dopamine deficiency with increasing relative glucose metabolism in the basal ganglia and limbic system. Furthermore, a more advanced stage of dopaminergic loss manifested in decreased metabolic connectivity within brain regions of the disease-related metabolic pattern of DLB, pronounced in the basal ganglia and limbic system. These findings clearly show that disturbed brain metabolism in particular regions is linked to extent of dopaminergic loss in DLB. As already proposed for PD and other atypical parkinsonian syndromes, the identification of metabolic network alterations at early stages of dopaminergic loss, preceding onset of motor symptoms, may serve as a supporting biomarker for diagnosis of DLB. ■

Acknowledgments: We are grateful to the European Dementia with Lewy Bodies consortium for this inspiring collaboration and intellectual exchange. We thank radiographers and technicians at all study centers for their invaluable support in data acquisition.

References

1. Barker WW, Luis CA, Kashuba A, et al. Relative frequencies of Alzheimer disease, Lewy body, vascular and frontotemporal dementia, and hippocampal sclerosis in the State of Florida Brain Bank. Alzheimer Dis Assoc Disord 2002;16:203–212.
2. Walker Z, Possin KL, Boeve BF, Aarsland D. Lewy body dementias. Lancet 2015;386:1683–1697.
3. McKeith IG, Boeve BF, Dickson DW, et al. Diagnosis and management of dementia with Lewy bodies: fourth consensus report of the DLB Consortium. Neurology 2017;89:88–100.
4. Walker Z, Moreno E, Thomas A, et al. Evolution of clinical features in possible DLB depending on FP-CIT SPECT result. Neurology 2016;87:1045–1051.
5. Morbelli S, Chincarini A, Brendel M, et al. Metabolic patterns across core features in dementia with lewy bodies. Ann Neurol 2019;85:715–725.
6. Bauckneht M, Arnaldi D, Nobili F, Aarsland D, Morbelli S. New tracers and new perspectives for molecular imaging in Lewy body diseases. Curr Med Chem 2018;25:3105–3130.
7. McKeith I, O'Brien J, Walker Z, et al. Sensitivity and specificity of dopamine transporter imaging with 123I-FP-CIT SPECT in dementia with Lewy bodies: a phase III, multicentre study. Lancet Neurol 2007;6:305–313.
8. Jellinger KA, Attems J. Does striatal pathology distinguish Parkinson disease with dementia and dementia with Lewy bodies? Acta Neuropathol 2006;112:253–260.
9. O'Brien JT, Colloby S, Fenwick J, et al. Dopamine transporter loss visualized with FP-CIT SPECT in the differential diagnosis of dementia with Lewy bodies. Arch Neurol 2004;61:919–925.
10. Walker Z, Jaros E, Walker RW, et al. Dementia with Lewy bodies: a comparison of clinical diagnosis, FP-CIT single photon emission computed tomography imaging and autopsy. J Neurol Neurosurg Psychiatry 2007;78:1176–1181.
11. Nicastro N, Garibotto V, Allali G, Assal F, Burkhard PR. Added value of combined semi-quantitative and visual [123I]FP-CIT SPECT analyses for the diagnosis of dementia with Lewy bodies. Clin Nucl Med 2017;42:e96–e102.
12. Nobili F, Arbizu J, Bouwman F, et al. European Association of Nuclear Medicine and European Academy of Neurology recommendations for the use of brain (18) F-fluorodeoxyglucose positron emission tomography in neurodegenerative cognitive impairment and dementia: Delphi consensus. Eur J Neurol 2018;25:1201–1217.
13. Morbelli S, Perneczky R, Drzezga A, et al. Metabolic networks underlying cognitive reserve in prodromal Alzheimer disease: a European Alzheimer disease consortium project. J Nucl Med 2013;54:894–902.
14. Caminiti SP, Tettamanti M, Sala A, et al. Metabolic connectomics targeting brain pathology in dementia with Lewy bodies. J Cereb Blood Flow Metab 2017;37:1311–1325.
15. Galvin JE, Price JL, Yan Z, Morris JC, Sheline YI. Resting bold fMRI differentiates dementia with Lewy bodies vs Alzheimer disease. Neurology 2011;76:1797–1803.
16. Kenny ER, Blamire AM, Firbank MJ, O'Brien JT. Functional connectivity in cortical regions in dementia with Lewy bodies and Alzheimer's disease. Brain 2012;135(Pt 2):569–581.
17. Peraza LR, Kaiser M, Firbank M, et al. fMRI resting state networks and their association with cognitive fluctuations in dementia with Lewy bodies. Neuroimage Clin 2014;4:558–565.
18. Peraza LR, Colloby SJ, Deboys L, O'Brien JT, Kaiser M, Taylor JP. Regional functional synchronizations in dementia with Lewy bodies and Alzheimer's disease. Int Psychogeriatr 2016;28:1143–1151.
19. Schumacher J, Peraza LR, Firbank M, et al. Functional connectivity in dementia with Lewy bodies: a within- and between-network analysis. Hum Brain Mapp 2018;39:1118–1129.
20. Ko JH, Lee CS, Eidelberg D. Metabolic network expression in parkinsonism: clinical and dopaminergic correlations. J Cereb Blood Flow Metab 2017;37:683–693.
21. Schindlbeck KA, Eidelberg D. Network imaging biomarkers: insights and clinical applications in Parkinson's disease. Lancet Neurol 2018;17:629–640.
22. Niethammer M, Tang CC, Ma Y, et al. Parkinson's disease cognitive network correlates with caudate dopamine. Neuroimage 2013;78:204–209.

23. Massa F, Arnaldi D, De Cesari F, et al. Neuroimaging findings and clinical trajectories of Lewy body disease in patients with MCI. Neurobiol Aging 2019;76:9–17.

24. Biundo R, Weis L, Bostantjopoulou S, et al. MMSE and MoCA in Parkinson's disease and dementia with Lewy bodies: a multicenter 1-year follow-up study. J Neural Transm (Vienna) 2016;123: 431–438.

25. Morbelli S, Chincarini A, Brendel M, et al. Metabolic patterns across core features in dementia with Lewy bodies. Ann Neurol 2019;85:715–725.

26. Albert NL, Unterrainer M, Diemling M, et al. Implementation of the European multicentre database of healthy controls for [(123)I]FP-CIT SPECT increases diagnostic accuracy in patients with clinically uncertain parkinsonian syndromes. Eur J Nucl Med Mol Imaging 2016;43:1315–1322.

27. Hammers A, Allom R, Koepp MJ, et al. Three-dimensional maximum probability atlas of the human brain, with particular reference to the temporal lobe. Hum Brain Mapp 2003;19:224–247.

28. Yakushev I, Hammers A, Fellgiebel A, et al. SPM-based count normalization provides excellent discrimination of mild Alzheimer's disease and amnestic mild cognitive impairment from healthy aging. Neuroimage 2009;44:43–50.

29. Brendel M, Kleinberger G, Probst F, et al. Increase of TREM2 during aging of an Alzheimer's disease mouse model is paralleled by microglial activation and amyloidosis. Front Aging Neurosci 2017;9:8.

30. Horwitz B, Duara R, Rapoport SI. Intercorrelations of glucose metabolic rates between brain regions: application to healthy males in a state of reduced sensory input. J Cereb Blood Flow Metab 1984;4: 484–499.

31. Burkhardt JM, Jin X, Costa RM. Dissociable effects of dopamine on neuronal firing rate and synchrony in the dorsal striatum. Front Integr Neurosci 2009;3:28.

32. Plenz D, Kital ST. A basal ganglia pacemaker formed by the subthalamic nucleus and external globus pallidus. Nature 1999;400: 677–682.

33. Chiba Y, Fujishiro H, Iseki E, Kasanuki K, Sato K. The cingulate island sign on FDG-PET vs. IMP-SPECT to assess mild cognitive impairment in Alzheimer's disease vs. dementia with Lewy bodies. J Neuroimaging 2019;29:712–720.

34. Celone KA, Calhoun VD, Dickerson BC, et al. Alterations in memory networks in mild cognitive impairment and Alzheimer's disease: an independent component analysis. J Neurosci 2006;26:10222–10231.

35. Borghammer P, Cumming P, Aanerud J, Gjedde A. Artefactual subcortical hyperperfusion in PET studies normalized to global mean: lessons from Parkinson's disease. Neuroimage 2009;45: 249–257.

36. Borghammer P, Jonsdottir KY, Cumming P, et al. Normalization in PET group comparison studies—the importance of a valid reference region. Neuroimage 2008;40:529–540.

37. Borghammer P, Chakravarty M, Jonsdottir KY, et al. Cortical hypometabolism and hypoperfusion in Parkinson's disease is extensive: probably even at early disease stages. Brain Struct Funct 2010; 214:303–317.

38. Ma Y, Tang C, Moeller JR, Eidelberg D. Abnormal regional brain function in Parkinson's disease: truth or fiction? NeuroImage 2009; 45:260–266.

39. Lozza C, Marie RM, Baron JC. The metabolic substrates of bradykinesia and tremor in uncomplicated Parkinson's disease. NeuroImage 2002;17:688–699.

40. Gardner RC, Boxer AL, Trujillo A, et al. Intrinsic connectivity network disruption in progressive supranuclear palsy. Ann Neurol 2013;73:603–616.

41. Morbelli S, Drzezga A, Perneczky R, et al. Resting metabolic connectivity in prodromal Alzheimer's disease. A European Alzheimer Disease Consortium (EADC) project. Neurobiol Aging 2012;33: 2533–2550.

Supporting Data

Additional Supporting Information may be found in the online version of this article at the publisher's web-site.